Electronic Supplementary Information

Flower-like porous BCN assembled by nanosheets for paclitaxel delivery

Haiyan Wang,‡[a] Congling Wang,‡[a] Yuxian Deng,[a] Yuxin Han,[a] Shuo Xiang, [a] Hanning Xiao [a] and Qunhong Weng *[a]

[a] College of Materials Science and Engineering, Hunan University, 2 Lushan S Rd, Changsha, 410082 P.R. China

*Corresponding author E-mail: wengqh@hnu.edu.cn (Q. Weng)

‡Authors contributed equally

1. Experimental

Chemicals

Boric acid (H_3BO_3), zinc nitrate hexahydrate (Zn $(NO_3)_2 \cdot 6H_2O$), and ammonium chloride (NH_4Cl) were purchased from Sinopharm Co. Ltd. Urea (CH_4N_2O) was purchased from Shanghai Bide Pharmaceutical Co. Ltd. 2-methylimidazole (2-Melim) purchased from Shanghai Yien Chemical Technology Co. Ltd. Anhydrous ethanol (EtOH) purchased from Tianjin Fuyu Fine Chemical Co. Ltd. Formaldehyde solution (37%) was purchased by McLean Biochemical Technology Co. Ltd. Paclitaxel (PTX) was purchased from Shanghai Meryer Biochemical Technology Co. Ltd. Cy5.5 was purchased from Shanghai Yuanye Biotechnology Co., LTD. Dulbecco's modified Eagle's culture medium (DMEM), penicillin-streptomycin (PS, double antibody solution), fetal bovine serum protein (FBS), trypsin and phosphate buffer solution (PBS) were purchased from Gibco. Cell proliferation test kit (CCK-8) was purchased from Shanghai Topscience Biotechnology Co. Ltd. LysoTracker Green fluorescent (λ_{Ex}=504 nm, λ_{Em}=511 nm) probe was purchased from Beyotime Biotechnology Co. Ltd.

Synthesis of ZIF-L

ZIF-L was prepared accordingly to previously reported work.[1] Briefly, dimethylimidazole (9.0 g) and ammonium chloride (1.0 g) were dissolved in 180 mL of deionized water, then Zinc nitrate hexahydrate (1.785 g, 20 mL) was added to the solution and stirred at room temperature (400 rpm) for 3 hours. The obtained solution was then centrifuged to obtain the precipitate, which was washed three times and dried in the oven at a temperature of 60 ^{o}C.

Synthesis of ZBCN

0.72 g of boric acid and 3.5 g of urea were dissolved in 50 mL of DI water and stirred continuously. 0.5g of ZIF-L powder was added to the solution and

stirred continuously at 50 °C for 4 hours. The solution was centrifuged and washed three times to obtain the precursor. Then, the precursor was annealed at 950 °C for 1 hour at a heating rate of 5 °C/min in a tube furnace in ammonia atmosphere to obtain the ZBCN. In addition, ZBCN-g was also prepared with the addition of glucose as a supplementary carbon source during the synthesis of precursor. ZBCN-uf was synthesized without using urea during the synthesis of precursor.

Preparation of PTX@ZBCN

Firstly, 2 mL of PTX EtOH solution was prepared with concentrations of 1.0, 1.5, and 2.0 mg mL^{-1}, respectively. ZBCN suspensions in water were also prepared by adding 2.0 mg of ZBCN in 2 mL DI water. Then, the ZBCN suspension was added to the PTX solution dropwise under stirring at 360 rpm. After stirring for 12 h, the PTX@ZBCN solid was collected by centrifugation at 11000 r min^{-1} and washed with DI water for 4 times.

Material characterizations

SEM and TEM images were obtained on TESCAN MIRA3 LMH and JEOL JEM-F200 microscope, respectively. Powder XRD were conducted on a Rigaku Miniflex 600 instrument. FTIR spectra were conducted on a Thermo Scientific Nicolet 10 in the range of 4000-400 cm^{-1}. XPS spectra were taken on Thermo Scientific K-Alpha. BET and pore structure analysis were performed on a JW-BK200C analyzer with the pore size distribution calculated based on a BJH model. UV-vis-NIR spectra were recorded using a SHIMADZU UV-2600 spectrophotometer. The Zeta potential and dynamic light scattering (DLS) of samples were measured on a Zetasizer Nano ZSP system (Malvern Instruments, Malvern, UK). Cell imaging was performed on a Motic AE31E-EF-INW microscopy.

Determination of drug loading capacity

To determine the loading capacity of PXT, the PTX@ZBCN was redispersed in 2 mL DI water. Then, 0.05 mL of dispersion was diluted in 1.95 mL EtOH and ultrasonicated for 5 min. The concentration of PTX solution was measured at 229 nm on a UV-vis spectrophotometer. By subtracting the background absorbance of the respective ZBCN solution, the concentration of PTX can be calculated based on the standard curve. The loading capacity of PTX was calculated as follows:

$$LC\% = \left(\frac{w_{PTX}}{w_{ZBCN}}\right) \times 100\% \quad (1)$$

Here, $LC\%$ represents the loading capacity of drugs, and w_{PTX} and w_{ZBCN} represent the weight of loaded PTX and initial weight of ZBCN, respectively.

In Vitro PTX Release

PTX@ZBCN suspension (containing 500 μg of PTX) was placed in a dialysis bag and immersed in 200 mL of PBS buffer (pH=5.6 and pH=7.4), and gently stirred at room temperature (120 rpm) for drug release studies. The UV absorption peak of the external solution of the dialysis bag at 229nm was tested at different times. The concentration of PTX was calculated according to the standard curve, and the drug release curve can be obtained finally.

Biocompatibility and in vitro anti-cancer assay

Mouse breast cancer cells (4T1) and human embryonic kidney cells (293T) were cultured in DMEM containing 10% FBS (GibcoTM), 1% antibiotic and antimycotic solution (GibcoTM) at 37 °C in a humidified atmosphere with 5% CO_2. 4T1 cells and 293T cells were cultured overnight in 96-well plates with a density of about 5×10^4 cells per well at 37 °C in a humidified atmosphere containing 5% CO_2. Then, the ZBCN suspensions were added to the culture media to make the final concentrations of 0, 6.25, 12.5, 25, 50, and 100 μg mL^{-1},

respectively, for the cytocompatibility test. After 24 hours of cell culture, CCK-8 kit was used to detect the cell viability. Similarly, the cytotoxicity of PTX and PTX@ZBCN suspensions was also evaluated by measuring the cell viability of the 4T1 cells co-cultured with the samples at different concentrations. Control groups were set and treated at the same conditions for all the viability tests except adding the same volume of PBS solution instead of samples.

Cell imaging and colocalization assay

10 μL of ZBCN and PTX@ZBCN solutions were incubated with cells for 24 h, and the final concentration of ZBCN and PTX@ZBCN were 50 μg mL^{-1} and 30 μg mL^{-1}, respectively. Then, the cells were washed twice with PBS to remove the attached samples. LysoTracker Green was subsequently added for co-incubation for additional 15 min. Finally, fluorescence images of the cells were recorded using an inverted fluorescence microscope under the required excitation wavelengths.

In vivo anti-tumor assay

All animal experiments were conducted following Hunan University's animal use and care guidelines. Female BALB/c mice (5-6 weeks old, ~18g) were purchased from Changsha Tianqin Biotechnology Co., Ltd. The tumor models were established by subcutaneous injection of 100 μL of 4T1 cell suspension (~5×10^7 cells) into BALB/c mice. 12 BALB/c mice were randomly divided into three groups (n=4) when the mice's tumor volumes grew to ~100 mm^3. They were intratumorally injected with free PTX and PTX@ZBCN solutions (the PTX dose is 5 mg kg^{-1}). Every mouse was subjected to an injection of dose drugs on day zero and day seven. While in the control group, PBS was injected into tumors instead. Body weight and tumor volume were measured every other day to evaluate the biological toxicity and anti-tumor performance of the drugs.

At the end of experiments, all the mice were euthanized using cervical dislocation.

Statistical analysis

All data are expressed as mean ± standard deviation. Students' t-test and one-way ANOVA method were used to assess the difference between groups by SPSS software. The difference was considered to be statistically significant at $p < 0.05$ (*$p < 0.05$, **$p < 0.01$, *** $p < 0.001$).

2. Preparation of sample suspensions

ZBCN, ZBCN-g, and ZBCN-uf are well dispersed in water, and the sample suspension exhibits the Tyndall effect under laser irradiation (Fig. S1a-b). And PTX@ZBCN are well dispersed in PBS (pH=5.6 and pH=7.4) and serum for 1 h, and the sample suspension exhibits the Tyndall effect under laser irradiation (Fig. S1c-d). The SEM images of their precursors and products are shown in Fig. S2a-f. The addition of glucose does not change the leaf shape of ZIF-L (Fig. S2a), therefore the final ZBCN-g product maintains a flower-like morphology similar to that of ZBCN (Fig. S2b). However, ZBCN-uf without the addition of urea was irregular fragmented particle rather than flower-like structure (Fig. S2c). It can be seen from Figure S2d-f that the precursors of ZBCN and ZBCN-g exhibit flower-like morphology, while the precursors of ZBCN-uf are irregular spheres. In addition, PTX@ZBCN still retains the flower-like morphology (Fig. S2g).

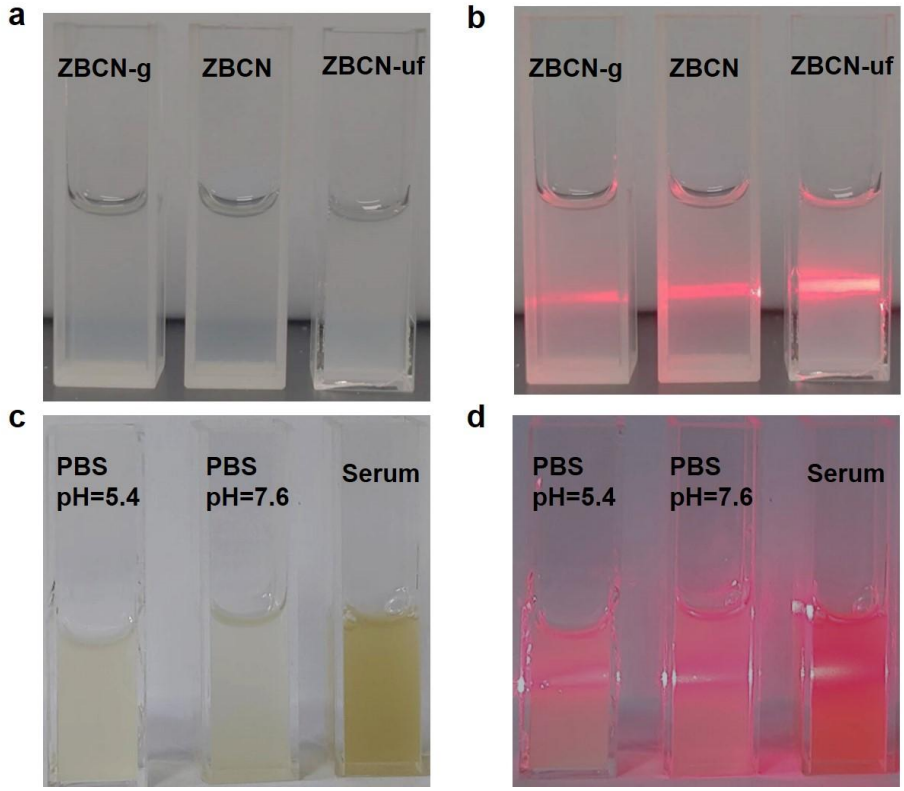

Fig. S1 (a) Photographs of ZBCN suspensions and (b) the corresponding Tyndall effect. (c) Photographs of PTX@ZBCN suspensions in different solutions and (d) the corresponding Tyndall effect.

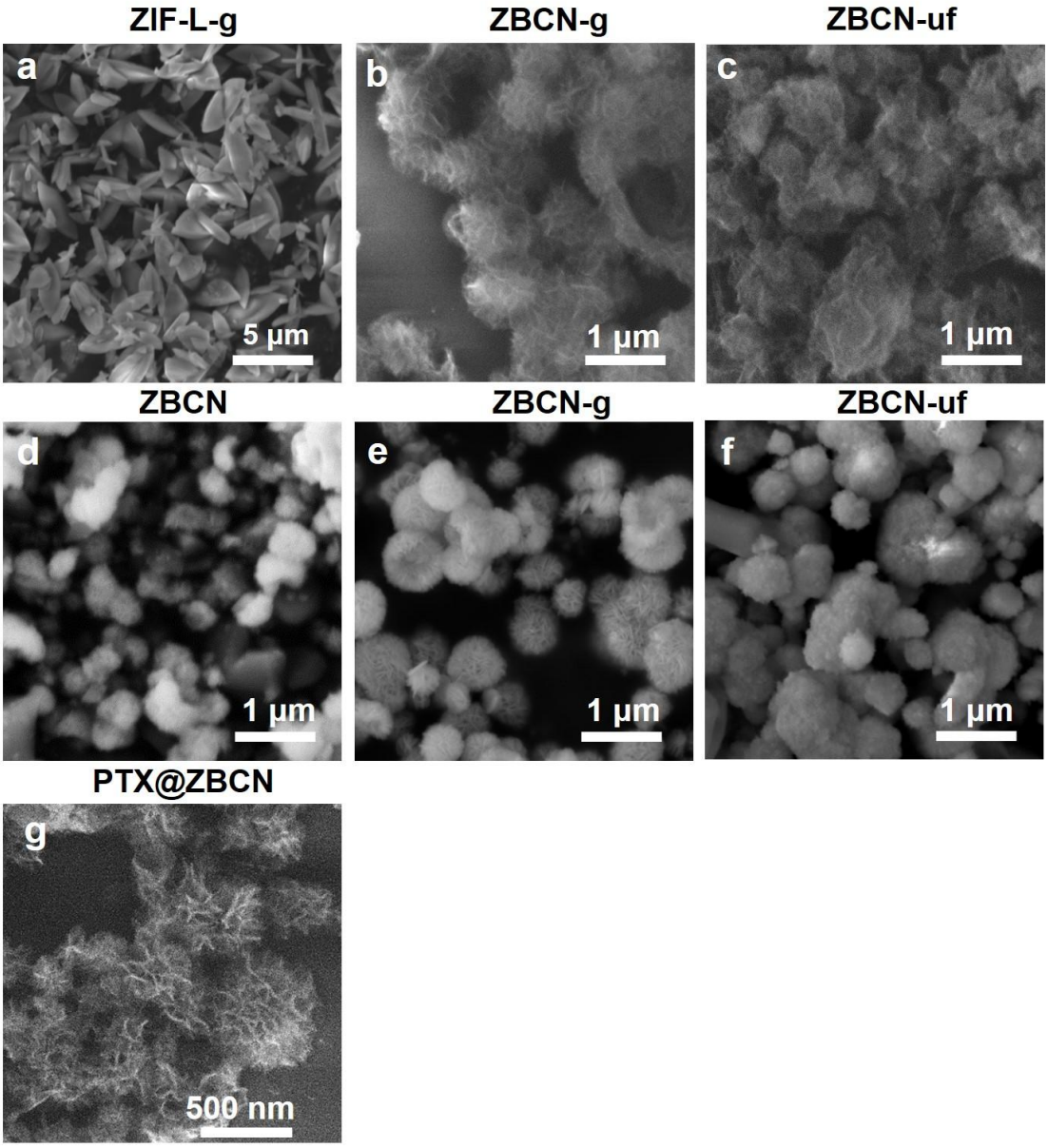

Fig. S2 (a) SEM image of ZIF-L. (b) SEM image of ZBCN-g and (c) ZBCN-uf. (d-f) SEM images of precursors for ZBCN, ZBCN-g and ZBCN-uf, respectively. (g) SEM image of PTX@ZBCN.

3. Dynamic light scattering analysis

The measured DLS average particle sizes of ZBCN, ZBCN-g, and ZBCN-uf are 158, 239, and 290nm, respectively. The Zeta potentials of ZBCN, ZBCN-g, and ZBCN-uf are -30, -39, and -33 mV, respectively (Fig. S3b). In addition, when the samples were loaded with PTX, their particle sizes increased to 189, 364, and 384 nm, respectively, and their potentials increased to -21, -28, and -27 mV, respectively (Fig. S3c-d).

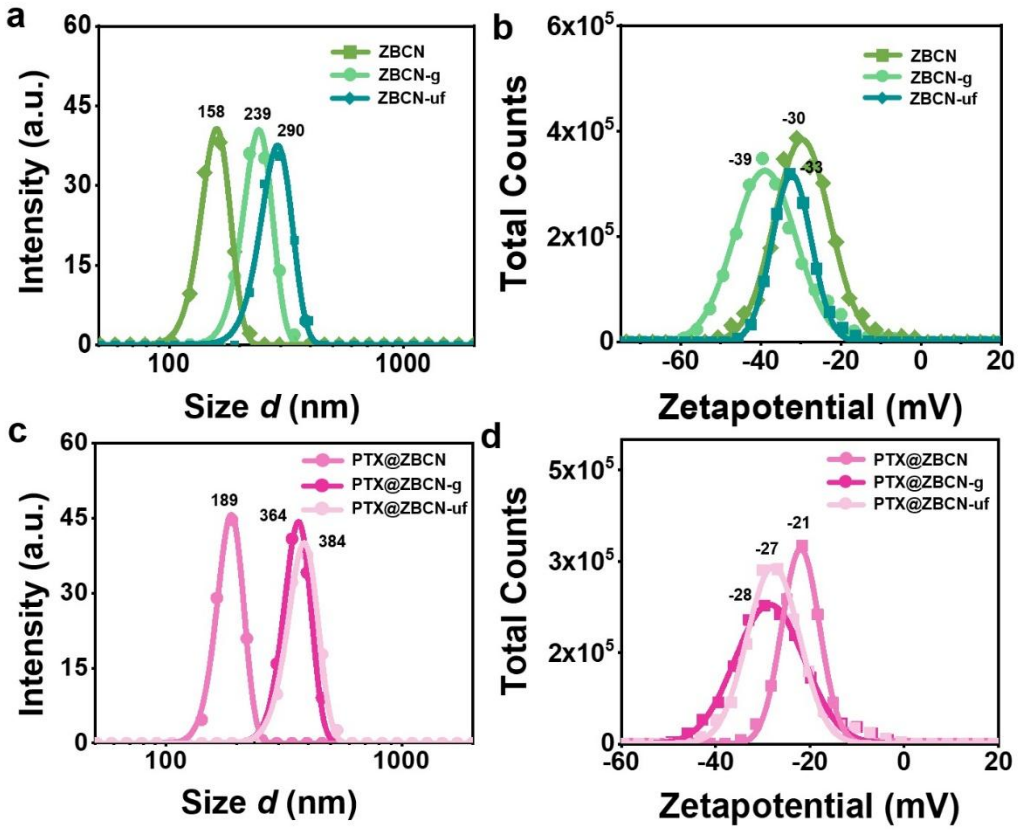

Fig. S3 (a,b) DLS and Zeta potential test results of the ZBCN samples before drug loading. (c,d) DLS and Zeta potential test results after drug loading.

4. Chemical structures

As shown in Fig. S4a, the XRD pattern of ZIF-L prepared by aqueous reaction is consistent with the previous report.[1] It can be observed that the characteristic diffraction peaks of ZIF-L still exist in the diffraction pattern of the ZBCN precursor (Fig. S4b), indicating that the crystal structure of ZIF-L has not been damaged with the addition of boric acid and urea precursors. It can be found from the XRD patterns that the characteristic peaks of ZBCN-g and ZBCN-uf (Fig. S4c) belong to typical h-BN phase. The FTIR spectra of the samples (Fig. S4d) show prominent peaks at 3433, 1384, 808, and 1596 cm^{-1}, which are the characteristic vibrational absorptions of -OH, B-N, B-N-B, and C=C bonds, respectively. From the XPS spectra shown in Fig. S4e, the addition of glucose or removal of urea can tune the contents of carbon and oxygen in the products, resulting in the changes of the overall atomic ratio (Fig. S4e). As shown in Fig. S4f, the peaks of C-C (284.6 eV), C-B (284.1 eV), C-N (285.6 eV), and C=O (287.61 eV) are fitted in the C1s spectrum. The B1s spectrum shows the primary B-C peak at 190.5 eV and B-N peak at 191.44 eV. The 398.04 eV and 399.06 eV peaks in the N1s spectrum correspond to the N-B and N-C bonds, respectively.[2, 3]

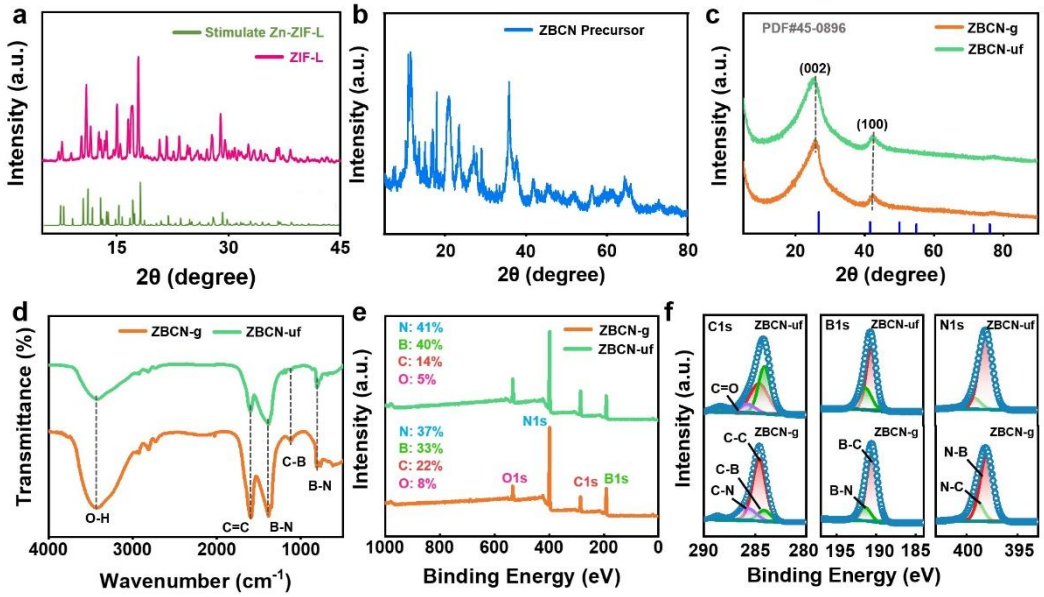

Fig. S4 XRD patterns of (a) ZIF-L and (b) ZBCN precursor. (c) XRD patterns of ZBCN-g and ZBCN-uf. (d) FTIR spectra of ZBCN-g and ZBCN-uf. (e) XPS survey spectra of ZBCN-g and ZBCN-uf. (f) XPS C1s, B1s and N1s spectra of ZBCN-g and ZBCN-uf.

5. Optical properties

The photoluminescence properties of the samples are shown in Fig. S5a-c. ZBCN and ZBCN-g have similar excitation and emission wavelengths with the Stokes shift of ~96 nm, which are larger and more advantageous than ZBCN-uf with the Stokes shift of ~28 nm. Besides, ZBCN-uf has the same emission wavelengths at 422 nm, but its excitation wavelength redshifts to 394 nm. The fluorescence images of the samples at different excitation wavelengths are shown in Fig. S6.

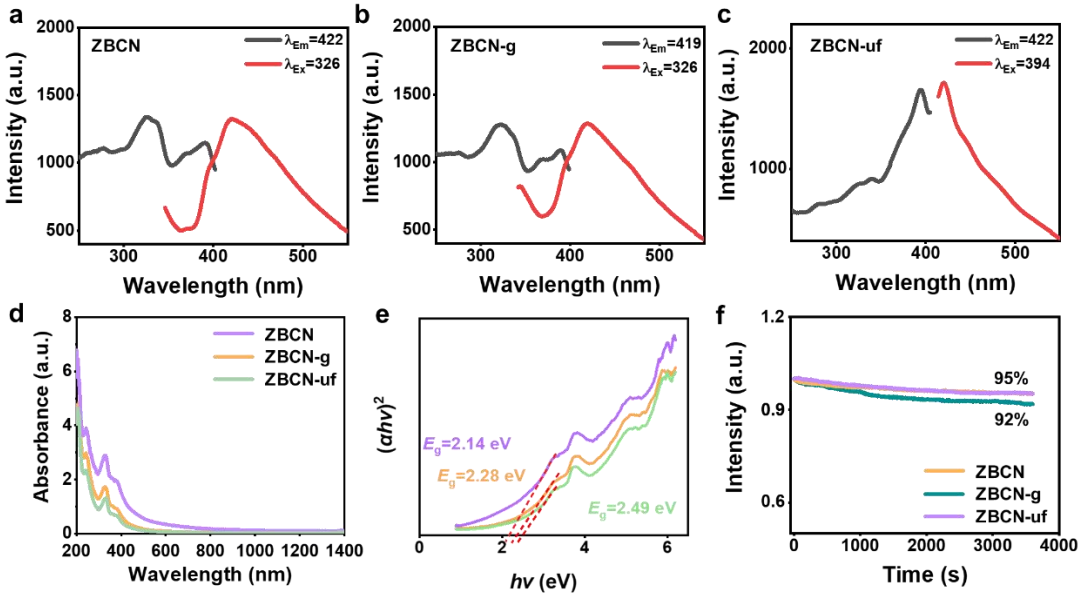

Fig. S5 (a-c) Photoluminescence spectra of ZBCN, ZBCN-g and ZBCN-uf. (d) UV visible spectra of ZBCN, ZBCN-g and ZBCN-uf. (e) PL stability measurements of ZBCN, ZBCN-g and ZBCN-uf under the irradiation of λ_{Ex}=326 nm and 394 nm.

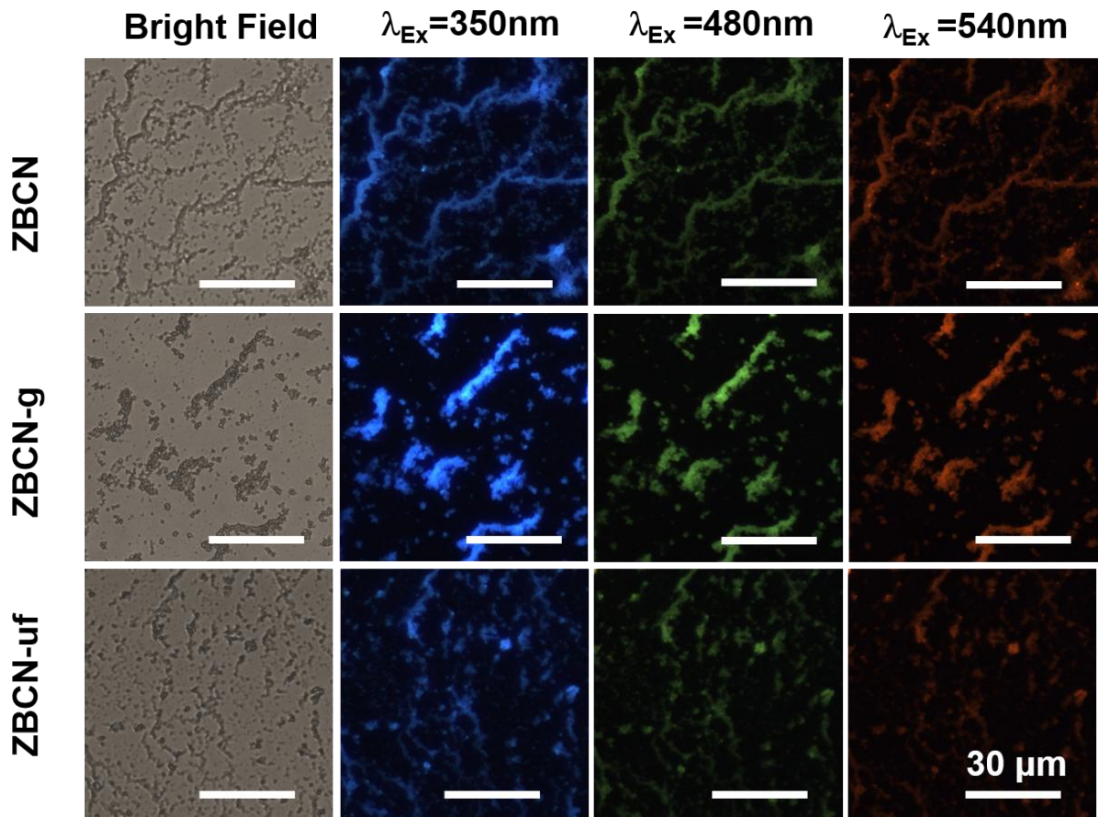

Fig. S6 Photographs of ZBCN, ZBCN-g and ZBCN-uf particles and the corresponding fluorescence images.

6. Cell viability

After incubating 4T1 cells and 293T cells with the sample for 24 hours, it was found that the cells grew well even at high concentrations of ZBCN. The cell viability is consistent with the results of CCK-8 assay, indicating that ZBCN has excellent cytocompatibility. The cell viability results of ZBCN-g and ZBCN-uf are shown in Fig. S8-9. The results of CCK-8 assay is consistent with the cell morphology, suggesting the good cytocompatibility of these samples.

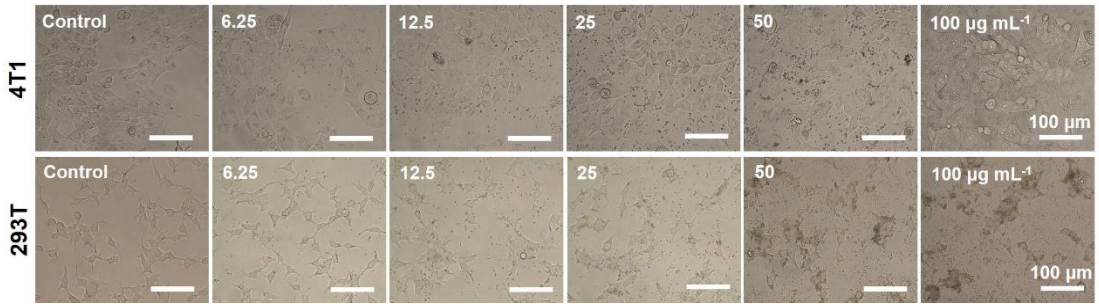

Fig. S7 Optical microscopic images of 4T1 cells and 293T cells co-cultured with ZBCN at different concentrations (control, 6.25, 12.5, 25, 50, 100 μg mL^{-1}) for 24 h.

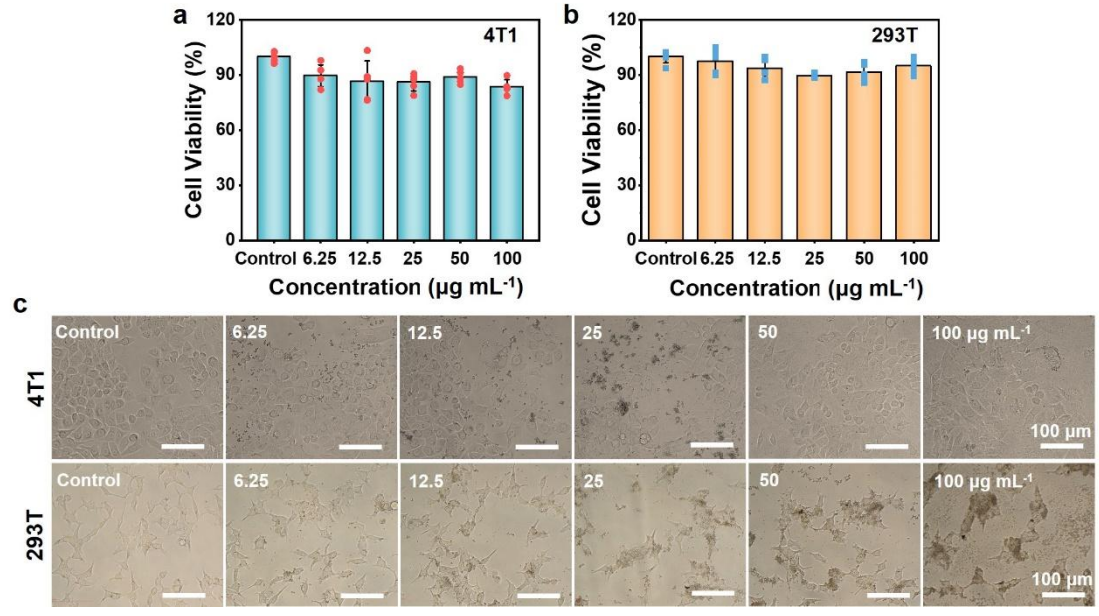

Fig. S8 (a,b) 4T1 and 293T cell viability of ZBCN-g at different concentrations after 24 h of co-incubation; (c) Optical microscopic images of 4T1 cells and 293T cells co-cultured with ZBCN at different concentrations (control, 6.25, 12.5, 25, 50, 100 μg mL^{-1}) for 24 h.

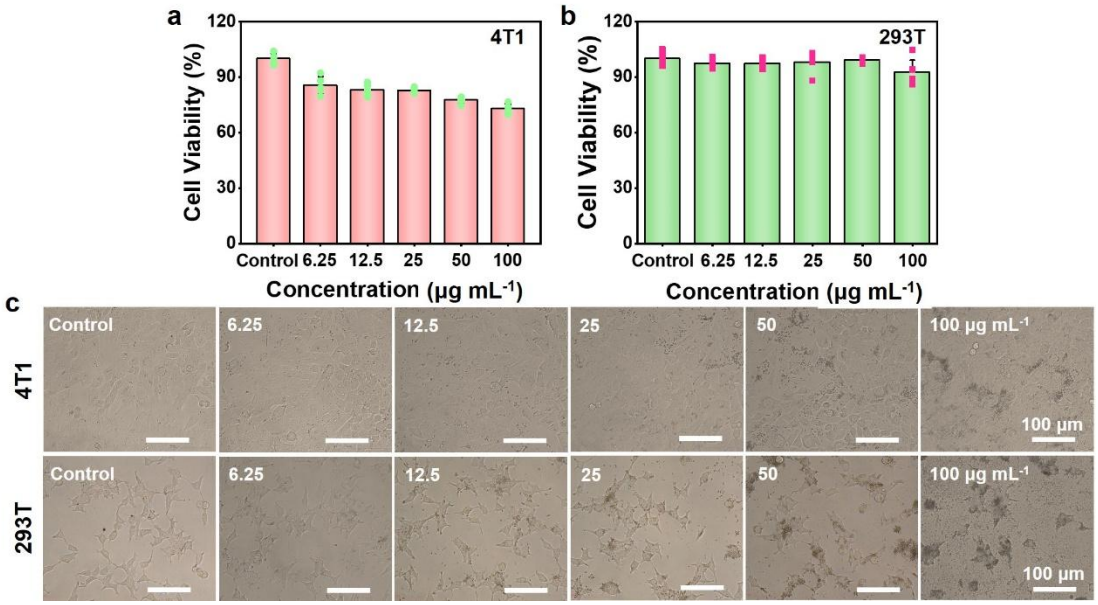

Fig. S9 (a,b) 4T1 and 293T cell viability of ZBCN-uf at different concentrations after 24 h incubation. (c) Optical microscopic images of 4T1 cells and 293T cells co-cultured with ZBCN at different concentrations (control, 6.25, 12.5, 25, 50, 100 μg mL^{-1}) for 24 h.

7. In vivo biodistribution and pharmacokinetics

The in vivo biodistribution and pharmacokinetics of ZBCN were studied by intravenous injection in mice (Fig. S10). With the presence of hydroxyl groups in ZBCN, Cy 5.5 is chemically combined with ZBCN through the esterification reaction using DMAP and DCC to form ZBCN-Cy 5.5. Six mice were injected with ZBCN-Cy 5.5 through the tail vein at a dose of 5mg kg^{-1}. The mice were euthanized by cervical dislocation at 1, 6, 12, 24, and 48 h, respectively. Then the heart, liver, spleen, lung, kidney and intestine were imaged by fluorescence imaging with excitation wavelength of 640 nm and detection wavelength range of 680 ~ 780 nm. The results showed that the ZBCN-Cy 5.5 rapidly accumulated mainly in the liver, lung and intestine of mice within 1 hour after the injection, with a minor distribution in the spleen. The fluorescence of spleen and intestine decreased rapidly within 12 h, and the fluorescence of liver and lung disappeared within 48 h. This experiment confirmed that the ZBCN accumulate rapidly in liver, lung, intestine and spleen through blood circulation, and finally metabolized within 2 days.

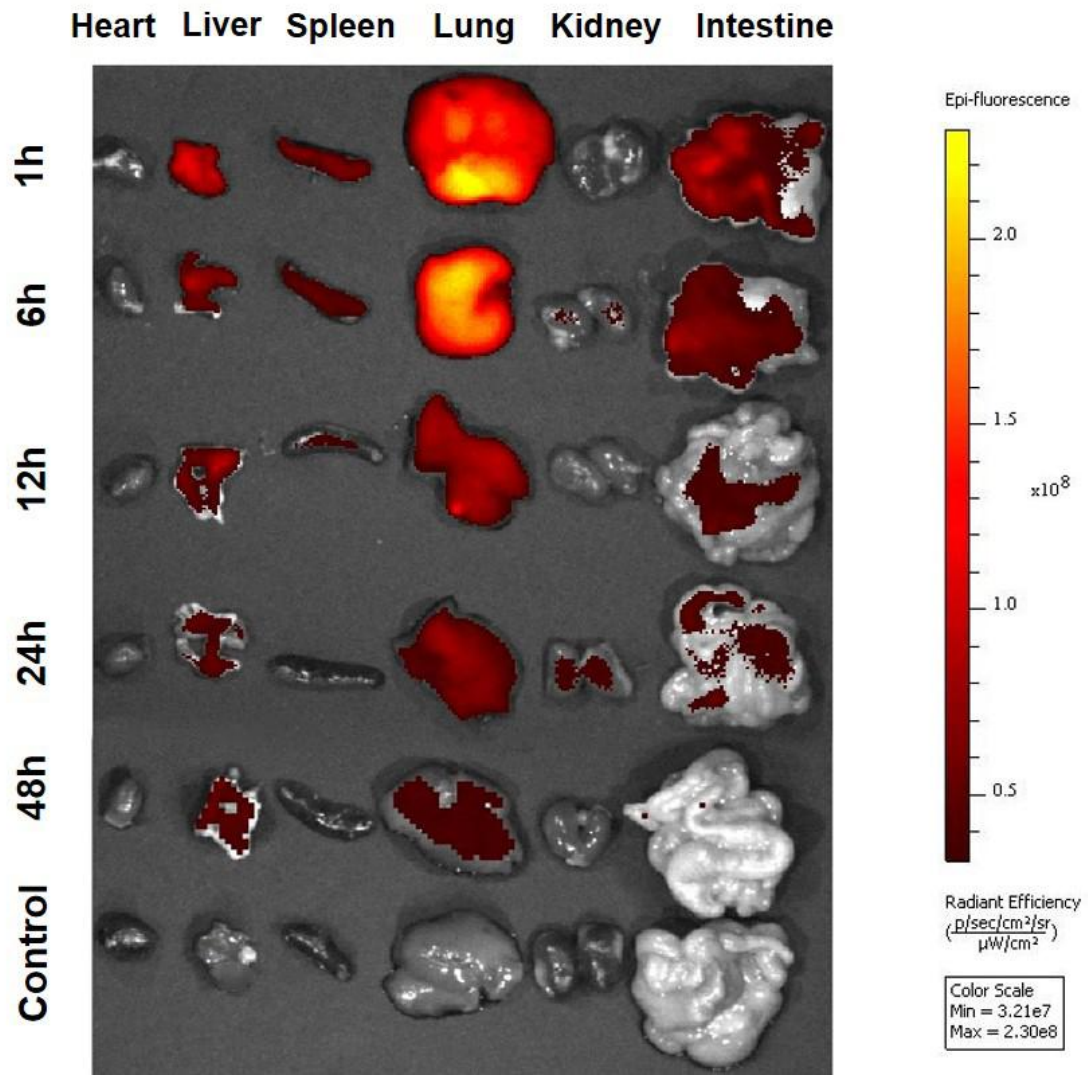

Fig. S10 Fluorescence images of mouse organs after injections of ZBCN-Cy5.5 for different time.

8. Drug loading and release

The drug loading capacity of the samples were determined by UV characteristic absorption peaks and standard working curves of PTX (Fig. S11). The PTX release curves of PTX@ZBCN and PTX@ZBCN-g are shown in Fig. S12.[4]

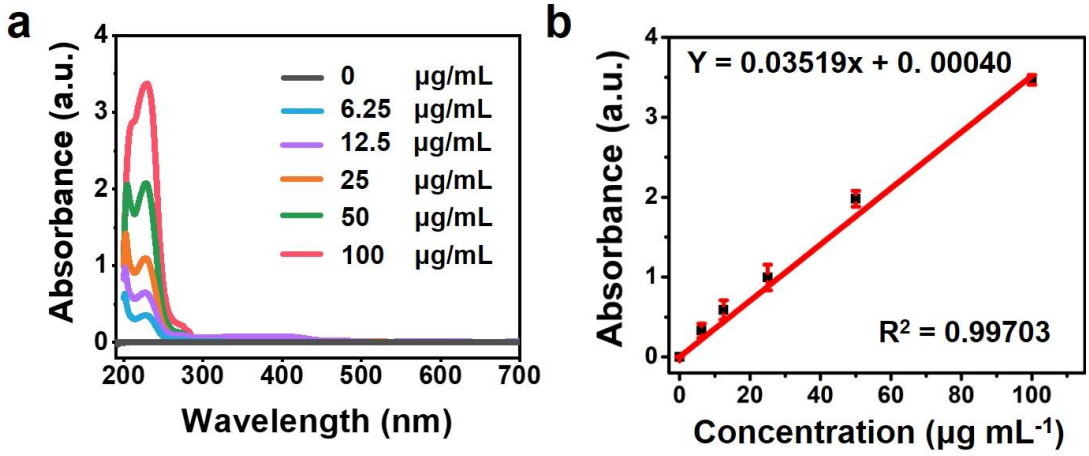

Fig. S11 (a) UV-vis absorption spectra of different concentrations of PTX solutions. (b) Standard working curve of PTX solutions (n = 3).

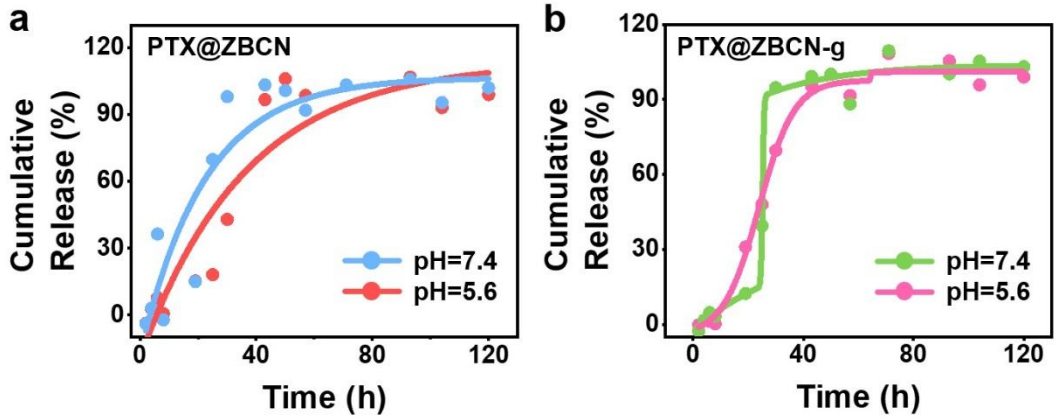

Fig. S12 (a,b) Release curves of PTX@ZBCN and PTX@ZBCN-g in PBS (pH=5.6 and pH=7.4).

9. PTX@ZBCN stability studies

The stability of the anticancer effects of PTX@ZBCN and PTX@ZBCN-g was studied, and it was found that the freshly prepared samples have better anticancer capabilities (Fig. S13a). When PTX@ZBCN-g was left to stand for 48 hours and then used for in vitro experiment, it was found that the cell viability increased to 52% at a sample concentration of 30 μg mL^{-1}, suggesting a significant decrease in the anticancer effect of the sample (Fig. S13b). Under the same conditions, PTX@ZBCN exhibits much better anticancer stability.

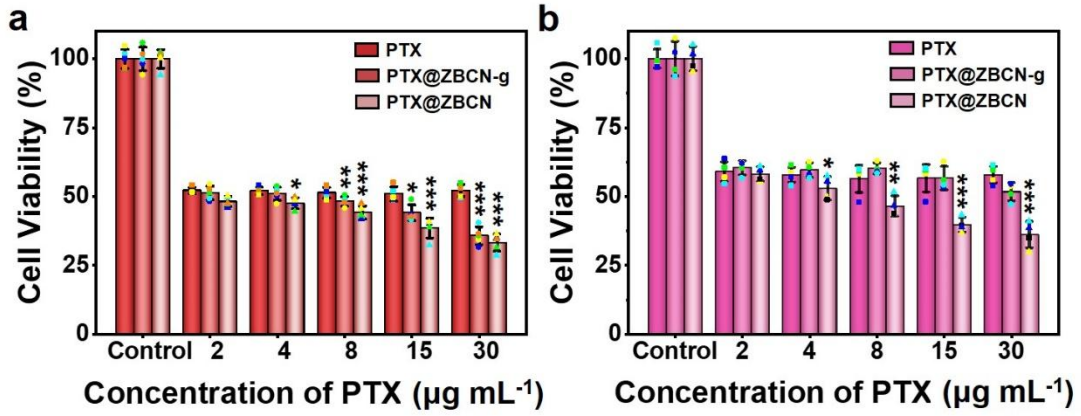

Fig. S13 Cell viability of free PTX, PTX@ZBCN-g and PTX@ZBCN at different PTX concentrations (control, 2, 4, 8, 15, 30 μg mL^{-1}) for 24 h. (a) Freshly prepared samples. (b) The samples used after standing for 48 hours.

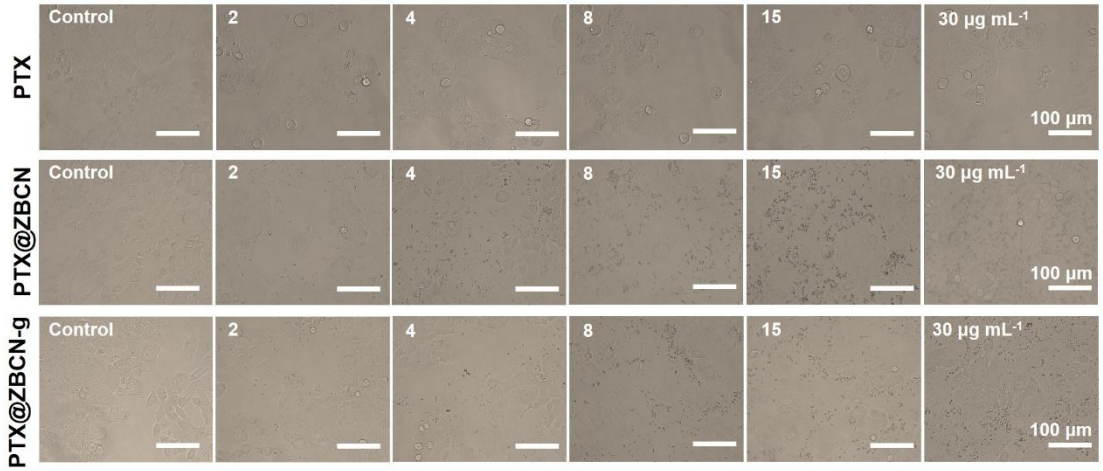

Fig. S14 Optical microscopic images of 4T1 cells co-cultured with free PTX, PTX@ZBCN-g and PTX@ZBCN (have been standing for 48 h) at different PTX concentrations.

10. PTX@ZBCN sustained release effect

Based on the sustained and slow release of PTX in PTX@ZBCN (Figure S12a), the PTX@ZBCN were studied on the long-term treatment of cancer cells (Fig. S15-S16). After 48 hours of co-incubation, the cell viability of the PTX@ZBCN group was 42% at a PTX dose of 30 μg mL^{-1}, while the cell viability of the free PTX group was 68%. This result confirms that the ZBCN can be used as a long-acting therapeutic drug carrier.

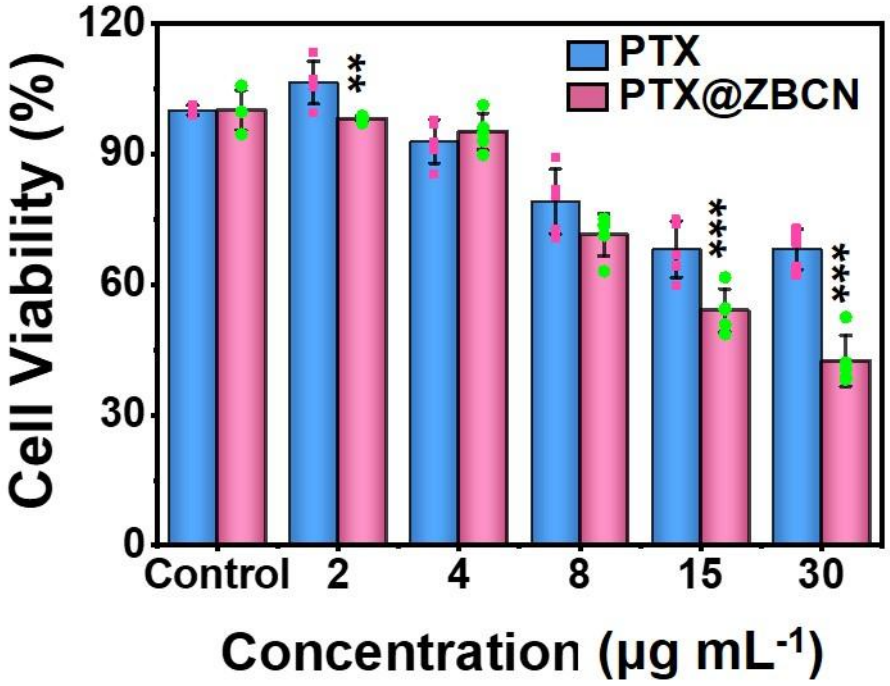

Fig. S15 The cell viability of free PTX and PTX@ZBCN at different PTX concentrations (control, 2, 4, 8, 15, 30 μg mL^{-1}) for continuous 48 h.

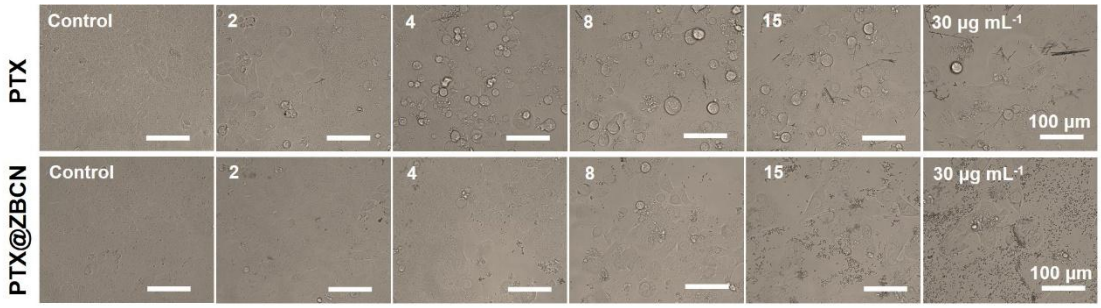

Fig. S16 Optical microscopic images of 4T1 cells co-cultured with free PTX and PTX@ZBCN at different PTX concentrations (control, 2, 4, 8, 15, 30 μg mL^{-1}) for continuous 48 h.

References

1 W. Xia, J. Tang, J. J. Li, et al., *Angew. Chem. Int. Ed.*, 2019, **58**, 13354-13359.
2 L. L. Zeng, Y. X. Han, Z. W. Chen, et al., *Adv. Sci.*, 2021, **8**, 2101184.
3 H. Yang, S. D. Gu, J. X. Li, et al., *Colloids Surf. B*, 2021, **198**, 111479.
4 G. Z. Han, S. Xiang, K. Jiang, et al., *J. Biomater. Appl.*, 2022, **37**, 1376-1383.